

Sequential steady state co-rotating dust vortices in sheared streaming plasma

Modhuchandra Laishram,^{1,*} Devendra Sharma,² and Ping Zhu^{1,3,4,†}

¹*CAS Key Laboratory of Geospace Environment and Department of Engineering and Applied Physics, University of Science and Technology of China, Hefei 230026, China*

²*Institute for Plasma Research, HBNI, Bhat, Gandhinagar 382428, India*

³*KTX Laboratory and Department of Engineering and Applied Physics, University of Science and Technology of China, Hefei 230026, China*

⁴*Department of Engineering Physics, University of Wisconsin-Madison, Madison, Wisconsin 53706, USA*

(Dated: February 5, 2022)

The 2D hydrodynamic model for a dust cloud confined in an axisymmetric toroidal system volumetrically driven by an unbounded streaming plasma is further extended systematically for different aspect-ratio of the bounded dust domain and a wide range of the kinematic viscosity. This work has demonstrated the interplay between inertial and diffusive transport processes for the structural changes of steady dust flow from symmetric into asymmetric nature in higher Reynolds number (Re) regimes where flow streamlines turn more circular and the structural bifurcation takes place through a threshold parameter. In agreement with many experimental observations, the steady vortex structure in highly nonlinear (i.e., high Re) regime is characterized by the critical transition into a new self-similar multiple co-rotating vortices, along with circular core region of single characteristics size and surrounded by strongly sheared layers filled with weak vortices near the boundaries. It is further revealed that the core region persists for a wide range of system parameters in the nonlinear regime and its characteristic size is mainly determined by the smallest distance between the confining boundaries. The threshold parameter, the vortex size, the strength, and the number of the self-similar co-rotating vortices mainly depend on the aspect-ratio of the bounded dust domain. These nonlinear solutions provide insight into the phenomena of the structural transition and coexistence of self-similar steady co-rotating vortices in dusty plasma experiments as well as many relevant complex driven-dissipative natural flow systems.

I. INTRODUCTION

Vortices are fundamental constituents of turbulence flow and collective dynamics in various driven-dissipative systems [1–5]. They have been observed in different shapes, sizes, strengths, and directions in varieties of laboratory dusty plasma experiments and biophysical complex flow systems [5–11]. And the existence of adjacent multiple counter-rotating vortices is intuitively explained by the shear nature of driving mechanisms [6, 12]. However, the appearance of self-similar co-rotating dust vortices reported in recent experiments with a background plasma flow of monotonic shear is rather counter-intuitive since a sharp dust flow shear layer is essentially present between two spatially adjacent co-rotating vortices, usually unexpected in steady fluid flow equilibria [8, 9, 11]. In such cases, the physics of single-fluid multiple vortices (like the Taylor-Couette vortices [13, 14]) may not be directly applicable to the volumetrically driven multiple-fluid cases such as those found in dusty plasma and biophysical complex systems [5, 8, 10].

The 2D hydrodynamic approach to the analysis of the dust vortex flow in plasma has been presented in a series of previous work [1, 12, 15, 16], in both linear and nonlinear regimes with the motivation to interpret the observations in laboratory dusty plasmas and those in

micro-gravity international space station (ISS) [6, 7]. The nonlinear analysis [1] briefly addresses the possible accessibility to secondary co-rotating vortices in the solutions it recovered in a square domain (AR=1) of dust confinement where the ratio of secondary to primary vortex remains limited to be $1 : (\sqrt{2} - 1)$. The possibility of self-similar co-rotating vortices was also discussed in the previous work predicting in advance the applicability of such solutions to some experiments where the recovery of co-rotating vortices are being explored [9, 10].

A partial freedom, allowed by the multiple equal-sized co-rotating vortex formations, from the bounded geometry of arbitrary shape is the subject of this paper. We discuss how an alternative convective mechanism facilitates the momentum transports and produces a rather non-intuitive and highly sheared arrangement of multiple adjacent co-rotating circular vortex flows observed in many recent experiments. For example, in the dusty plasma experimental work, Kil-Byoung Chai *et al.* (2016) [8] reported recovery of two adjacent co-rotating and counter-rotating poloidal vortices due to the presence of ion density gradient and the gradient of ion ambipolar velocity. They also observed the structural transition of the dust cloud into multiple vortices when the plasma density exceeds a critical value n_i^* . Further, in the series of recent experiments carried out by M. Choudhary *et al.* (2018) [9, 10], who has analyzed dust dynamics in a domain of higher aspect-ratio $L_z/L_r \approx 3$ to 5, indeed observed the structural transition from a single to co-rotating dust vortices of equal size by changing the applied discharge power through a threshold value P^* . Fur-

* modhu@ustc.edu.cn

† pzhu@ustc.edu.cn

ther, in some cases, they also observed variation in the number of co-rotating vortices at different cross-sections of the elongated 3D dust cloud in an inhomogeneous rf-plasma. In addition to this, apart from dusty plasma i.e., in the biophysical complex fluid flows, Nivedita et al. (2017) [5] have observed similar kind of structural changes and transition into multiple co-rotating vortices through a threshold in Dean number D^* in microfluidics systems such as spiral microchannels for cell sorting and micromixing devices. Here, D is a modified form of Re taking into account of aspect-ratio of the flow system. This work demonstrates a critical phenomena in term of an instability arising from the imbalance between flow pressure and velocity gradient near the boundary.

Although these observations have been reported in part, the actual physical interpretations for the steady vortex structural changes why the flow trajectory turns more circular with increasing the convective transport is not well understood. Then, the physics of the persistence of self-similar multiple co-rotating vortices, and the roles of aspect-ratio of the flow domain in the laboratory dusty plasma experiments are not discussed explicitly. Further, the phenomena of the steady dust vortex changes in characteristic size, numbers, strength, and direction of the self-similar multiple vortices remain unclear in the experiments, but the observations indicate that a combination of the dynamic regime and the aspect-ratio of the flow domain plays an important role in determining the vortex size and overall flow structure. Therefore, in this present work, we emphasize mostly on the effect of aspect-ratio, by extending the previous nonlinear analysis in the fixed domain of aspect-ratio unity ($AR=1$) [1] to different aspect-ratio of the flow domain and varying a wide range of kinematic viscosities. The present work provides a more complete analysis and characterization of dust vortex dynamics where a sequence of self-similar co-rotating vortices are obtained in the domain of different aspect-ratios ($AR=2, 3$) relevant to recent experiments.

The manuscript is organized as follows. In Sec. II, we recall the 2D hydrodynamic model for the bounded dust flow in streaming plasma from the previous analysis [16], which is followed by the characterization of system parameters for the dynamic regime in Sec. III. Then, the qualitative effects of domain aspect-ratio and kinematic viscosity (or Re) are discussed in Sec. IV. Further, we examine some of the recent results in dusty plasma experiments and other complex fluids system using our model in Sec. IV C. Summary and conclusion is presented in Sec. V.

II. 2D NONLINEAR HYDRODYNAMIC MODEL

Similar to the previous analysis [1, 16], we consider a nearly incompressible dust fluid confined in an axisymmetric toroidal system along with an unbounded flowing plasma. The geometry of bounded dust fluid is very similar to that of recent experiments where a toroidal

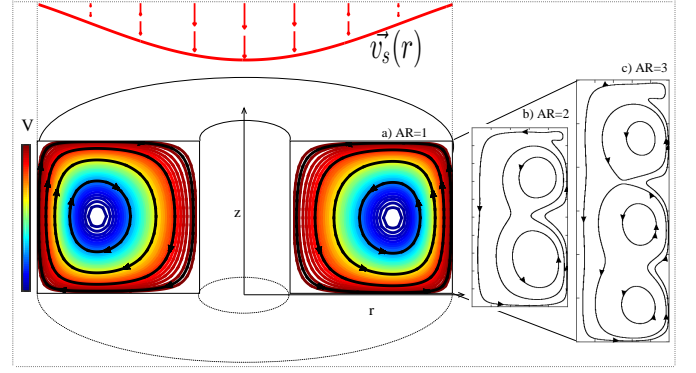


FIG. 1. Schematic representation of the dust cloud confined in an azimuthally symmetric torus by the effective potential $V(r, z)$ and driven by the shear ions field $v_s(r, x)$ interspersing through the bounded dust cloud, also demonstrating the steady-state dust vortex structure in nonlinear regimes for various aspect-ratio ($AR = L_z/L_r$) of the confined domain.

dust cloud flowing in the poloidal direction in a glow discharge plasma [6]. For computational simplicity, the poloidal cross-section of the axisymmetric torus is simplified as a rectangular domain as illustrated schematically in Fig 1. The dust fluid is confined by an effective potential $V(r, z)$ in the toroidal region where $0 < r/L_r < 1$, $-1 < z/L_z < 1$, and symmetric along $\hat{\phi}$, which can vary the size ($AR = L_z/L_r$) of dust confining domain, where the boundary serves as the equipotential line for the perfect confinement.

Then, using the stream function-vorticity formulation discussed in the previous work [1, 16], the dynamics of the dust flow that is incompressible, isothermal, and has a finite viscosity, is governed by the modified Navier-Stokes equations where the sheared ion drag and the friction from the stationary background neutral fluid can suitably be accounted as non-conservative momentum source and sink as follows [17],

$$\nabla^2 \psi = -\omega, \quad (1)$$

$$(\mathbf{u} \cdot \nabla) \omega = \mu \nabla^2 \omega - \xi(\omega - \omega_s) - \nu \omega. \quad (2)$$

Here, $\psi \hat{\phi}$ is the stream function giving incompressible dust flow velocity $\mathbf{u} = \nabla \times \psi \hat{\phi}$ in the 2D rz -plane, $\omega \hat{\phi} = \nabla \times \mathbf{u}$ is the corresponding dust vorticity, μ is the dust kinematic viscosity, ξ is the coefficient of ion drag acting on the dust, and ν is the coefficient of friction generated by the stationary neutral fluid [18–20]. Further, ω_s is the external vorticity source from the unbounded background flows. In a real system, any non-zero shear field such as $\nabla \times u_{i(n)}$, $(\nabla Q_d \times \mathbf{E})$, $(\nabla u_{i(n)} \times \nabla n_{i(n)})$ and $(\nabla T_{i(n)} \times \nabla n_{i(n)})$ of the complex background flow and their combinations can be driving mechanisms and contribute to the source of vorticity ω_s , because the coefficient ξ , ν , and μ depends on the state of the system [8, 18–21]. Here, Q_d is dust charge, \mathbf{E} is effective electric field along the streaming ions, and the subscript $i(n)$ represents the background ion (neutral). The overall combi-

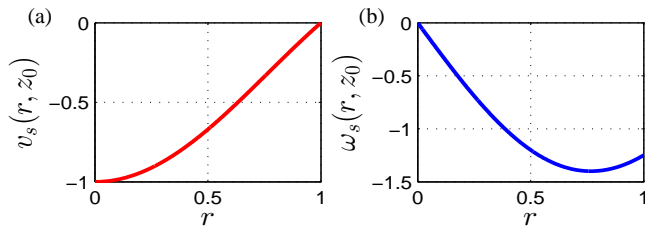


FIG. 2. Profiles of the external (a) driver velocity v_s , and the corresponding (b) driver vorticity ω_s which are uniform along axial \hat{z} and azimuthal $\hat{\phi}$ directions.

nation of charged dust and background plasma is quasi-neutral and the highly mobile background electrons and ions are in thermal equilibrium even though it interacts and intersperses through the confined dust fluids. Therefore, the steady equilibrium shear ions vorticity field ω_s in Eqn (2) is valid for representing the dominant ion drag interaction with the bounded dust dynamics [16].

III. CHARACTERIZATION OF THE BOUNDED DUST FLUID SYSTEM

Now, the set of equations (1)-(2), represent the steady state of the driven dust fluid for any dynamical regime defined by the system parameters ξ , ν , μ , the driving field ω_s , and the boundary conditions. A perfect slip, partial slip, and no slip are some of the very common boundary conditions encountered in dusty plasma. These equations are solved subjected to similar boundary conditions and numerical technique adopted from the previous work [1, 16].

For the main driving field, i.e., the vertically streaming sheared ions directed along $-\hat{z}$ ($v_r = 0$) is considered, motivated by various experiments [6, 10]. The radial profile of the streaming ions have a radial shear nature of the single natural mode of the nonplanar system as given in Eqn. (3), (also plotted in Fig 2), such that it maintains maximum velocity at the inner radial boundary ($r = r_1 \approx 0$) and minimum velocity at the external confining boundary ($r = L_r$) of the bounded domain.

$$v_z = U_c + U_0 J_0 \left(\alpha_m \frac{r - r_1}{L_r - r_1} \right). \quad (3)$$

Here U_c represents an offset, and U_0 is the strength of radial variation of the ions flow. The radial mode number α_m represents the zeros of corresponding ion velocity profile coinciding with the external boundary location L_r . The entire analysis is done using the same driver velocity $v_z(r, z)$ and its corresponding vorticity $\omega_s(r, z) = \nabla \times v_z$ profile as in the previous work [1].

Now, for the system parameters, the solutions presented here correspond to a typical laboratory glow discharge argon plasma with micron size dust, along with parameters $n \simeq 10^9 \text{ cm}^{-3}$, $T_e \simeq 3\text{eV}$, $T_i \simeq 1\text{eV}$, and shear ions are streaming with the value U_0 equivalent to the fraction of the ion acoustic velocity $c_s = \sqrt{T_e/m_i}$.

Then, using the radial width of the confined domain L_r and streaming shear ions velocity strength U_0 as the ideal normalization units, the value of ion drag coefficient and neutral collision frequency can be estimated as $\xi \sim 10^{-4} U_0/L_r$ and $\nu \sim 10^{-3} U_0/L_r$, respectively [18–20]. Further, for a typical system, $L_r \sim 10 \text{ cm}$, the range of kinematic viscosity μ can similarly be chosen to be $\mu \sim 6 \times 10^{-4} U_0 L_r$ which corresponds to small Reynolds numbers ($\text{Re} \simeq 1$) of the dust flow consistent with the linear viscous regime [1, 12, 22].

IV. FLOW STRUCTURE DEPENDENCE ON ASPECT-RATIO OF THE BOUNDED DOMAIN

In the previous analytical work [12], it has demonstrated that the vortex structure in the low velocity or linear regimes is mainly determined by the scale introduced by the external driving fields and the geometry of the bounded domain. However, in the high-velocity nonlinear regime [1, 16], the steady flow structure is again influenced mainly by the dynamical regime in addition to the scales introduced by the geometry of the bounded domain. Thus, the flow structural change continuously in response to the increase in strength of advective transport process $(\mathbf{u} \cdot \nabla)\omega$ relative to the diffusive transport process $\mu \nabla^2 \omega$. Along with this structural changes in the nonlinear regime, the nonlinear structure bifurcation takes place through a threshold value μ^* [1], and the flow turns into a more complex self-organized structure consisting of multiple vortices of varying shape, size, strength, and direction.

In terms of scales available in the flow system, the diffusive transport process mainly depends on the characteristic length across the flows L_\perp , whereas convective transport depends on characteristic length $L_\parallel (\approx u/u')$ along flow streamlines. Therefore, the nonlinear structural changes with diffusive coefficient μ can also be described in terms of the variation in characteristic length L_\perp relative to the L_\parallel and vice versa, which are correlated to the changes in aspect-ratio ($AR = L_z/L_r$) of the bounded flow domain. Thus, the aspect-ratio of the bounded flow has an important role in determining the steady-state flow structure. The dependence of bounded flow characteristics on the domain aspect-ratio can also be visualized in a simple way as follow. For the volumetrically driven system of aspect-ratio $AR (= L_z/L_r)$ with a driver having the fixed monotonic shear scale L_r and uniform dissipative neutrals at the background, the vertically streaming ions can intersperse through the bounded fluid for maximum range up to L_z . Therefore, for higher AR ($L_z \gg L_r$), the shear ions flow can interact or transfer relatively larger momentum to the confined dust in comparison to the case of small aspect-ratio ($L_z \leq L_r$), and hence the dust cloud retains more and more momentum from the source ions. As a consequence, the structural changes with system parameters are very different in various aspect-ratio of the bounded flow domain.

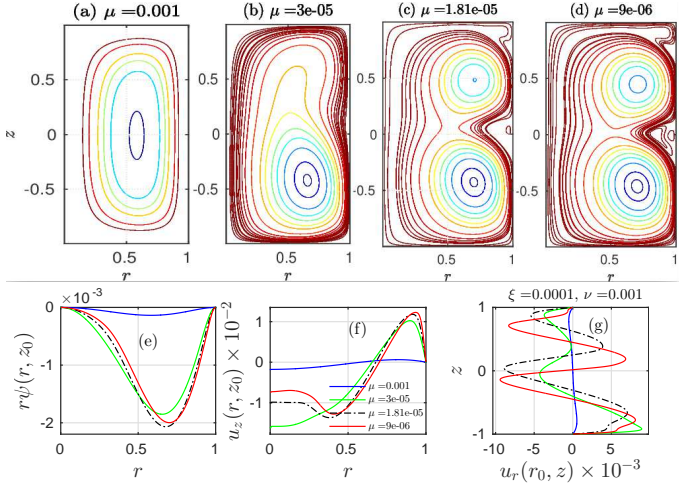


FIG. 3. Streamlines for the steady bounded dust flow in r - z cross-section of $AR = 2$ for varying (a) $\mu = 10^{-3}U_0L_r$, (b) $\mu = 3 \times 10^{-5}U_0L_r$ (c) $\mu = 1.8 \times 10^{-5}U_0L_r$ and (d) $\mu = 9 \times 10^{-6}U_0L_r$ respectively having fixed other system parameters $\xi = 10^{-4}U_0/L_r$, $\nu = 10^{-3}U_0/L_r$. The corresponding cross-section profiles for (e) $r\psi(r, z_0)$, (f) $u_z(r, z_0)$ and (g) $u_r(r_0, z)$ passing through the center of the primary vortex.

In the following, we examine the steady state dust flow structural changes for a wide range of kinematic viscosity μ in different aspect-ratio of the bounded dust flow domain.

A. Steady dust flow structure in the confined domain of aspect-ratio $AR = 2$

A series of steady state dust flow structure in a confining domain of aspect-ratio $AR = 2$ are shown in Fig. 3, for the wide range of kinematic viscosity μ evolving from linear to nonlinear regimes without changing any other system parameters. As discussed in the recent work [16], the flow structure in the confined domain in the case of highly viscous regime $\mu \sim 10^{-3}U_0L$ (or $Re \leq 10$) is symmetric and elongated circulations as shown in Fig. 3(a). When the diffusive coefficient reduces to $\mu \sim 3 \times 10^{-5}U_0L$ (or $10 \leq Re \leq 40$), the vortex structure turns into asymmetric about the centerline, the center of circulation drifted axially downward and radially outward to a new position in the new state as shown in Fig. 3(b). The observed structural changes with varying μ from symmetric to asymmetric developing highly shear layers near the boundary is the beginning of the nonlinear effect arises in the flow [23, 24]. Then the nonlinear effect becomes more strengthened with further reduces in the diffusive coefficient up to $\mu \sim 10^{-5}U_0L$ or less (i.e., increase in $Re \geq 80$), and as a consequence, the nonlinear structural bifurcation takes place through a critical value $\mu^* \approx 1.81 \times 10^{-5}U_0L_r$ giving multiple co-rotating vortices of the bounded dust cloud in the flow domain [1].

Now, in a steady circulating flow with fixed sources and sinks, the fluid element retains more and more momentum along the closed paths with a decrease in the diffusive transport process. Therefore, the flow trajectory turned more circular since the circular path allows to keep maximum angular velocity ($\approx 2\omega$) without a significant change in the angular momentum of the whole system. Thus, the new vortex structure in the highly angular velocity regime is characterized by the emergence of a circular core region of single scale i.e., the characteristic size of the circular core (s), on which the Prandtl-Batchelor theorem is satisfied ($\frac{\partial \omega}{\partial \psi} \approx 0$ means $\mu \oint \nabla^2 u \cdot d\mathbf{l} \approx 0$) [1, 25]. This means the steady core region of uniform vorticity surrounded by highly shear collar layer is free from viscous dissipation, and hence it persists for a wide range of system parameters in the non-linear regime. This gives the physical condition for the persistence of circular core region in the driven system. The characteristic core size s is mainly determined by the dominant scale introduced either by the shear driving field or the smallest distance between the confining boundaries. Thus, in the case of highly nonlinear flow in larger domain aspect-ratio ($L_z/L_r \gg 1$), whose scale is larger than the core size s , a part of the highly sheared boundary layer detaches from the actual boundary and extends deeper into the interior along the collar of core vortex. It begins to act as a virtual core boundary providing a vanishing flow velocity condition similar to the actual external boundary. As a consequence, the flow structure turns into a system of self-similar multiple co-rotating vortices having a uniform core region and surrounded by the corresponding highly sheared layers filled with small-scale weak vortices as shown in Fig. 3(c). Further, we observe a steady increase in the size and strength of small-scale vortices with decreasing μ as shown in Fig. 3(d), until the flow gets stabilized into more stable identical structures with its own scale ratio of near unity ($\approx 1:1$), which used to be $1:(\sqrt{2}-1)$ in the case of domain aspect-ratio of unity ($AR=1$) [1].

The structural changes in the flow fields can also be visualized from the variation in cross-section profile of the streamline potential $r\psi$ and the dust flow velocity profiles (u_r, u_z) through the center of the primary vortex (r_0, z_0) as shown in Fig. 3(e), (f) and (g) respectively. Here, all $r\psi$, u_x , and u_y strengthen with the decreasing diffusive coefficient μ . The radial shift of the center of vortex in the new flow structure can be observed from the extremum of the radial $r\psi$ profile in Fig. 3(e). The structural bifurcation that develops the extended virtual boundary around the core vortex can be demonstrated from the variation of $u_z(r, z_0)$ in Fig. 3(f). Here, u_z at $r = r_1 (\approx 0)$ shows a maximum up to the critical value μ^* then begins to drop below its value in the interior (around the core vortex) despite that the driver strength always maximum at $r = r_1$. Furthermore, the radial component of the dust flow velocity $u_r(z, r_0)$ shows periodic variation that vanishes at $z \sim 0$ such that the line $z \sim 0$ begins to behave like the virtual boundary as shown in

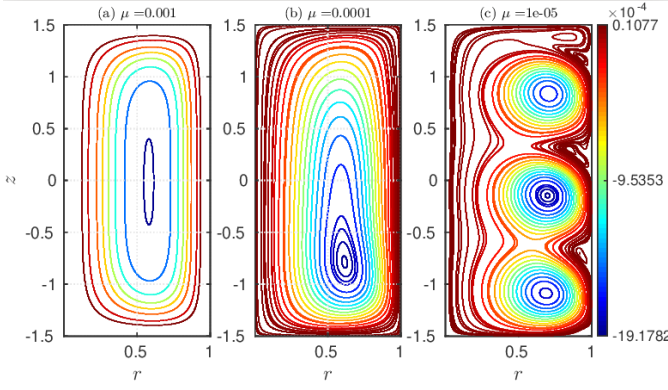


FIG. 4. Streamlines for the steady bounded dust flow in the r - z plane of $AR = 3$ for varying (a) $\mu = 10^{-3}U_0L_r$, (b) $\mu = 10^{-4}U_0L_r$, (c) $\mu = 10^{-5}U_0L_r$ respectively having fixed other system parameters $\xi = 10^{-4}U_0/L_r$, $\nu = 10^{-3}U_0/L_r$.

Fig. 3(g). Both the u_x and u_y tend to a saturated stable state having a uniform single shear scale between two equidistant opposite peaks indicating the emergence of the high-speed collar layer or virtual boundary (separatrix) which separate the core region from the highly shear boundary regions.

B. Steady dust flow structure in the confined domain of aspect-ratio $L_z : L_r = 3$

The analysis for the flow structural changes is extended further to a confinement domain of aspect-ratio $L_z/L_r = 3$. The variation in the circulating flow structure is demonstrated with the same external driver v_z , the same system parameters ξ , ν , and varying only the kinematic viscosity μ such that the corresponding effective Reynolds number varies from linear to highly nonlinear regime ($Re \simeq 0.1$ to 100). A series of streamlines pattern in the axisymmetric r - z toroidal plane are shown in Fig. 4. Here, as discussed in the above section IV A, the flow structure in the linear regime $\mu = 10^{-3}U_0L_r$ (or $Re \leq 10$) is again symmetric and elongated circulations that closely resembles the geometry of the bounded domain as shown in Fig. 4(a). When the varying parameter decreases to $\mu \approx 10^{-4}U_0L_r$ (or $Re \geq 20$), the vortex flow converges to a new asymmetric structure as shown in Fig. 4(b). And further decrease in the parameter to $\mu \approx 10^{-5}U_0L_r$ produces the qualitative topological change through the nonlinear structural bifurcation about a critical kinematic viscosity μ^* [1]. And as a consequence, the circulating flow pattern makes transition to a new self-organized steady flow structure having a sequence of three self-similar co-rotating circular vortices, each having a nearly uniform vorticity core region with a characteristic size s relevant to the smaller scale of the domain L_r ($\ll L_z$), and bounded by the shear layers filled with weak vortices as shown in Fig. 4(c). In addition to this, Fig. 5 displays the corresponding changes in diffu-

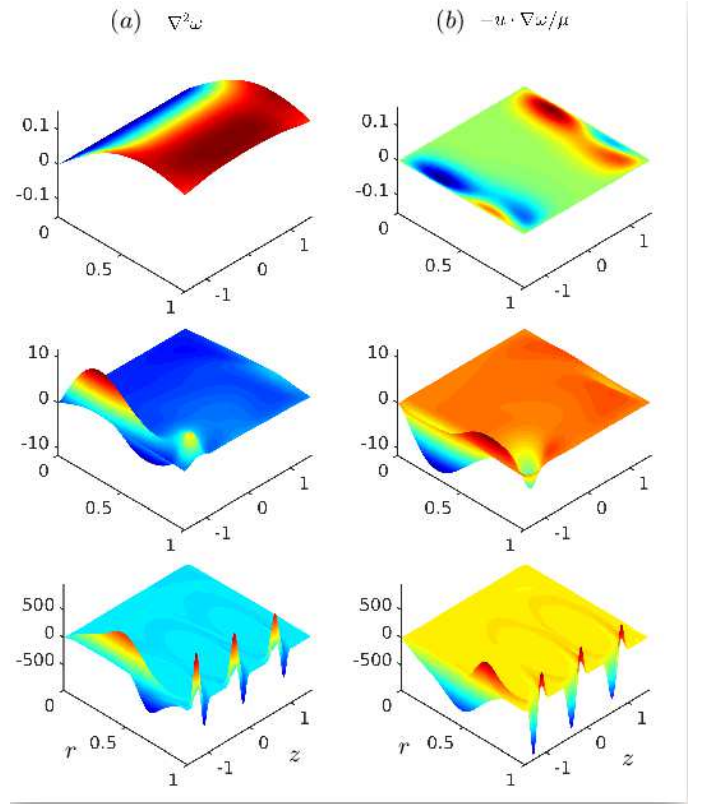


FIG. 5. Relative strengths of (a) the diffusive transport and (b) the convective transport plotted from top to bottom for the values of dust viscosity $\mu = 1 \times 10^{-3}U_0L_r$, $1 \times 10^{-4}U_0L_r$, and $1 \times 10^{-5}U_0L_r$ respectively having fixed other system parameters $AR = 3$, $\xi = 10^{-4}U_0/L_r$, and $\nu = 10^{-3}U_0/L_r$.

sive transport process $\mu\nabla^2\omega$ (1st column) relative to the convective process of vorticity $(\mathbf{u} \cdot \nabla)\omega$ (2nd column) with decreasing the kinematic viscosity μ . Diffusive transport dominant in linear regime turns into a balance of both convective and diffusive flow in the nonlinear regime, while the changes in non-conservative source and sink of vorticity are negligible. It demonstrates that the changes in the steady dust fluid vortex structure are mainly contributed by the interplay between inertial and diffusive transport process from its sources to the homogeneous sink present in the form of stationary background fluid.

Further, one more remarkable observation in the present analysis is that the bounded dust cloud retains much more momentum than any other cases of aspect-ratio $L_z/L_r \ll 3$ for the same conditions of other dynamic factors. Therefore, the threshold parameter for the structural bifurcation in the present case of $L_z/L_r = 3$ is found to be $\mu^* \approx 8 \times 10^{-5}U_0L_r$, whereas $\mu^* \approx 1 \times 10^{-5}U_0L_r$ for $L_z/L_r = 2$ and ($\mu^* \approx 5 \times 10^{-6}U_0L_r$ in case of $L_z/L_r = 0.5$). Moreover, the formation of a sequence of stable identical vortices are observed with higher μ^* in the case of larger aspect-ratios $L_z/L_r \gg 3$. And for the dimensions where $L_z/L_r \gg 1$ but not an integer multiple of L_r say 1.5, 2.5 etc., a partially developed elongated and

weak vortices are visible in addition to the integer numbers of fully grown vortices, which closely resemble the small vortices seen in the upper corner of Fig. 3(d) and Fig. 4(c). This analysis further demonstrates the condition for the existence of self-similar multiple co-rotating vortices in a driven-dissipative bounded flow system, of which the characteristic size, numbers, and strength of the multiple vortices depend on the aspect-ratio of the bounded flow domain. In the above whole analysis, the observed scale of dust velocity $u \approx 10^{-3}U_0$ agree with the experimental observations of $u \sim 0.1 - 6$ cm/sec in high Reynolds regime while shear ions are streaming with $c_s \sim 27$ cm/sec in various typical dust vortex flow experiments in both laboratory as well as microgravity space station [6, 7, 10].

C. Relevant steady state co-rotating vortices in laboratory experiments

Now, we discuss the correspondence between our result on multiple co-rotating vortices and the similar observation in various recent experiments where the physics of the transition to an apparently higher velocity shear configuration remained not well understood or unsupported by an adequate physics model. Here we particularly focus on three recent examples, namely the observations reported by Kil-Byoung Chai *et al.* (2016) [8], M. Choudhary *et al.* (2018) [9, 10], and in one of the cases in biological complex fluids namely, Nivedita *et al.* (2017) [5]. All these experiments recovered the above transition in some form by variation of the system parameter such as ξ , μ , ν , and boundary conditions in our model.

In the experiments by Kil-Byoung Chai *et al.* [8], vortex motion of a bounded dust cloud in an rf-discharge plasma is analyzed in presence of various non-conservative ion-drag forces such as $(\nabla u_i \times \nabla n_i)$ and $(\nabla T_i \times \nabla n_i)$ exerted on the dust cloud. As a combined effect of all sources, a system of axisymmetric toroidal multiple vortices including two adjacent co-rotating and counter-rotating vortex flows are recovered for a typical plasma density and temperature profile. It also observed that the multiple vortices appear only when the plasma density (i.e. ion density) exceeds through a critical value n_i^* . Furthermore, the observed secondary vortices are less distinct or weaker in strength than the primary vortex. From the perspective of our model, the changes in ion density n_i can be interpreted as variation in the ξ or the drive strength U_0 , whereas the variation in vortex size and strength can also be understood as an effect of changing the aspect-ratio of the bounded domain as discussed in above section IV B.

We now discuss another example of dusty plasma experiments by M. Choudhary *et al.* [9, 10] who observed steady multiple co-rotating vortices in an extended dust cloud confined in an inhomogeneous diffused rf-plasma. They first observed variation in the number of co-rotating vortices at the different cross-section of the extended dust

cloud. Then they also observed the structural transition from a single to a state of multiple co-rotating dust vortices at a particular cross-section by changing the applied discharge power or voltage through a threshold value. In the experiment, the dissipative instability due to the non-zero $\nabla Q_d \times \mathbf{E}$ in addition to the ion drag forces arising from the inhomogeneous background plasma [1, 21] are reported as the main source of vorticity. Here Q_d is the charge on the dust particle, and \mathbf{E} is the effective electric field along the ions flow direction. Further, using the Vaulina *et al.* model [26], they interpreted the vortex characteristic size in terms of the diffusive scale, and its ratio to the overall dust cloud dimension gives the number of the sustainable vortices in the driven system.

The explanation on the co-rotating character of the vortex, however, remains an open question, since the purely diffusive transport mechanism prescribes multiplicity of vortex only with the spatially non-monotonic driver [6, 12, 15]) and thus excludes the possibility of formation of any adjacent co-rotating vortices in such system. In this relation, the explanation provided by the Choudhary *et al.* although referred to author's work [15], dealing with the linear diffusive regime but completely ignores the nonlinear convective solutions presented in the subsequent publication [1], duly relating them to the recovery of co-rotating vortices in flow domain of AR=1. Note that it is the nonlinear regime that is exactly relevant to their observations of adjacent self-similar co-rotating dust vortices which are not explained by only the diffusive transport, i.e., without including the convective nonlinear effects. Again, from the perspective of our model, the changes in the applied discharge power can be modeled by varying ξ or the drive strength U_0 , whereas the variations in vortex size and number can also be understood as an effect of the aspect-ratio of the bounded domain as discussed in the above sections IV A and IV B.

For the sake of completion, and more importantly to highlight the strong relationship between macroscopic observations in dusty plasmas to the microscopic dynamics in complex biological fluids, we now discuss the observation by Nivedita *et al.* [5] who reported the similar kind of structural changes and transition of the single vortex into multiple co-rotating vortices in various spiral rectangular microchannels of different aspect-ratio for cell sorting and micromixing devices. They provided systematic experimental as well as numerical insight into the phenomena of the structural transition by the variation of Dean number through a threshold value D^* . They have demonstrated the critical phenomena in term of an instability called Dean instability arising from the imbalance of flow pressure and velocity gradient near the boundary. In comparison to our model, pressure corresponds incompressible dust flow velocity \mathbf{u} , the changes in Dean number D directly correlate to the variation of μ for the bounded flow domain having a fixed aspect-ratio (AR), and the Dean instability is another feature of the nonlinear structural bifurcation through the threshold param-

eter. Moreover, they have demonstrated the variation of the threshold value D^* for varying the aspect-ratio, similar to the recovery of various critical μ^* in different aspect-ratios in above analysis of section IV A and section IV B. This work actually highlights the fact that dusty plasma can be one of the easily realizable prototypes for the study of various driven-dissipative complex flow systems that can self-stabilize by making a critical transition to a self-similar state.

V. SUMMARY AND CONCLUSIONS

We have extended and systematically analyzed the nonlinear solutions of the 2D hydrodynamic model for the dynamics of volumetrically driven bounded dust cloud in an unbounded streaming plasma [1] for different aspect-ratio (AR) of bounded domain and a wide range of the kinematic viscosity (μ). This analysis has demonstrated the interplay between convective and diffusive transport processes in determining the steady vortex structure of the bounded dust cloud for the wide range of Reynolds numbers from linear to a highly nonlinear regime. This analysis also gives the insight that the effective Reynolds number of the bounded flow system with fixed source and sink of momentum can be controlled through the aspect-ratio of the flow domain in addition to the fluid's diffusive coefficient μ . Therefore, the vortex structural changes from the linear to highly nonlinear flow regimes are analyzed in a larger domain of AR=2 and AR=3. The series of steady flow structure in case of AR=2, has clearly demonstrated the nonlinear effects of structural changes from symmetric into asymmetric nature in the nonlinear regime that exhibits regions of localized acceleration in the flow field. Moreover, it reveals the physical reason for the flow trajectory turns into more circular and the nonlinear structural bifurcation takes place about a threshold parameter μ^* . Thus the new vortex structure in highly nonlinear regime is characterized by the critical transition into new self-similar multiple co-rotating vortices having circular core region of single characteristics size s on which the viscous dissipations is negligible (uniform vorticity) and hence it would persist for a long range of system parameters in the nonlinear regime. It has further revealed that the size s is mainly determined by the dominant scale introduced either by the shear driving field or the smallest distance between the con-

fining boundary. Thus, for the cases of ($AR \gg 1$), the multiple co-rotating vortices get stabilized with a scale ratio of near unity ($\approx 1 : 1$), which were scale ratio of $1 : (\sqrt{2} - 1)$ in case of aspect-ratio of unity (AR=1) [1]. Further, the series of the steady flow structure in case of AR=3 displays clearly how the structure changes with varying the flow domain's aspect-ratio and kinematic viscosity. Thus, the driven flow system allows to retain more momentum either through an increase in AR or decreasing μ . As a consequence, the threshold parameter μ^* for the structural bifurcation decrease in the bounded domain of larger AR. Additionally, this work also demonstrated the impact of the system parameters in determining the characteristic size, shape, strength, and numbers of the self-similar co-rotating vortices in many of relevant driven-dissipative flow systems.

The whole analysis of unusual structural dependence on the dynamical parameters including the AR of the flow domain is relevant to many of recent dusty plasma experiments as well as biological complex fluid flows [5, 8, 10]. This signifies the fact that the proposed structural bifurcation through the threshold parameter is another aspect of the Dean instability or dissipative instability reported in the real experimental systems. This nonlinear threshold phenomenon may associate with shear instabilities which can be investigated further by extending the same analysis to real-time dependence in well-defined parameter regimes.

VI. ACKNOWLEDGMENTS

Author L. Modhuchandra acknowledge Prof. Abhijit Sen and late Prof. P. K. Kaw, Institute for Plasma Research, India, for the invaluable supports, encouragements, scientific suggestions, and criticisms. The research was supported by the State Administration of Foreign Experts Affairs - Foreign Talented Youth Introduction Plan Grant No. WQ2017ZGKX065, the National Magnetic Confinement Fusion Program of China under Grant Nos. 2014GB124002 and 2015GB101004. Author P. Zhu also acknowledges the support from U.S. DOE grant Nos. DE-FG02-86ER53218 and DE-FC02-08ER54975. The work used the resources of Supercomputing Center of University of Science and Technology of China.

-
- [1] M. Laishram, D. Sharma, P. K. Chattopadhyay, and P. K. Kaw, *Phys. Rev. E* **95**, 033204 (2017).
 - [2] J. C. McWilliams, *J. Fluid Mech.* **219**, 361385 (1990).
 - [3] M. Schwabe, S. Zhdanov, C. R  th, D. B. Graves, H. M. Thomas, and G. E. Morfill, *Phys. Rev. Lett.* **112**, 115002 (2014).
 - [4] P. Meunier, S. L. D  zs, and T. Leweke, *C. R. Phys.* **6**, 431 (2005), aircraft trailing vortices.
 - [5] N. Nivedita, P. Ligrani, and I. Papautsky, *Scientific Reports* **7**, 44072 (2017).
 - [6] M. Kaur, S. Bose, P. K. Chattopadhyay, D. Sharma, J. Ghosh, Y. C. Saxena, and E. T. Jr., *Phys. Plasmas* **22**, 093702 (2015).
 - [7] V. N. Tsytovich, G. Morfill, U. Konopka, and H. Thomas, *New J. Phys.* **5**, 66 (2003).

- [8] K.-B. Chai and P. M. Bellan, Phys. Plasmas **23**, 023701 (2016).
- [9] M. Choudhary, S. Mukherjee, and P. Bandyopadhyay, Phys. Plasmas **24**, 033703 (2017).
- [10] M. Choudhary, S. Mukherjee, and P. Bandyopadhyay, Phys. Plasmas **25**, 023704 (2018).
- [11] M. Mondal, S. Sarkar, S. Mukherjee, and M. Bose, Contributions to Plasma Physics **58**, 56 (2017).
- [12] M. Laishram, D. Sharma, and P. K. Kaw, Phys. Rev. E **91**, 063110 (2015).
- [13] G. I. Taylor and R. S. F., Philos Trans R Soc London A **223**, 289 (1923).
- [14] J. T. Stuart, “Taylor-vortex flow: A dynamical system*,” <https://epubs.siam.org/doi/pdf/10.1137/1028104>.
- [15] M. Laishram, D. Sharma, and P. K. Kaw, Phys. Plasmas **21**, 073703 (2014).
- [16] M. Laishram and P. Zhu, Physics of Plasmas **25**, 103701 (2018).
- [17] L. Landau and E. Lifshitz, *Fluid Mechanics*, v. 6 (Elsevier Science, 2013).
- [18] M. S. Barnes, J. H. Keller, J. C. Forster, J. A. O’Neill, and D. K. Coultas, Phys. Rev. Lett. **68**, 313 (1992).
- [19] S. A. Khrapak, A. V. Ivlev, G. E. Morfill, and H. M. Thomas, Phys. Rev. E **66**, 046414 (2002).
- [20] A. V. Ivlev, S. A. Khrapak, S. K. Zhdanov, G. E. Morfill, and G. Joyce, Phys. Rev. Lett. **92**, 205007 (2004).
- [21] M. Laishram, D. Sharma, P. K. Chattopdhyay, and P. K. Kaw, AIP Conference Proceedings **1925**, 020028 (2018).
- [22] G. Salin and J.-M. Caillol, Phys. Rev. Lett. **88**, 065002 (2002).
- [23] S. Mitic, R. Sütterlin, A. I. H. Höfner, M. Thoma, S. Zhdanov, and G. Morfill, Phys. Rev. Lett. **101**, 235001 (2008).
- [24] T. H. Hall and E. Thomas, IEEE Transactions on Plasma Science **44**, 463 (2016).
- [25] G. K. Batchelor, J. Fluid Mech. **1**, 177190 (1956).
- [26] O. S. Vulina, A. A. Samarian, O. F. Petrov, B. W. James, and V. E. Fortov, New J. Phys. **5**, 82 (2003).